NUMERICAL WELL MODEL FOR NON-DARCY FLOW THROUGH ISOTROPIC POROUS MEDIA

R.E. EWING, R. LAZAROV, S.L. LYONS, D.V. PAPAVASSILIOU, J. PASCIAK, AND G. QIN

ABSTRACT. Numerical simulation of fluid flow in a hydrocarbon reservoir has to account for the presence of wells. The pressure of a grid cell containing a well is different from the average pressure in that cell and different from the bottomhole pressure for the well (Peaceman, [18]). This paper presents a study of grid pressures obtained from the simulation of single phase flow through an isotropic porous medium using different numerical methods. Well equations are proposed for Darcy flow with Galerkin finite elements and mixed finite elements. Furthermore, high velocity (non-Darcy) flow well equations are developed for cell-centered finite difference, Galerkin finite element and mixed finite element techniques.

1. INTRODUCTION

The difficulty in modeling wells in a field scale numerical simulation of a reservoir is that the region where pressure gradients are largest ($\mathcal{O}$(1-10ft)) is closest to the well and is typically much smaller than the spatial scale of the associated computational grid cell ($\mathcal{O}$(10-1000ft)). Using local grid refinement around the well can alleviate this problem but can severely restrict the timestep size of the simulation. Futhermore, the pressure calculated by numerical methods in the well block (or blocks sharing the well as a corner point) is substantially different from the flowing bottom-hole pressure of the modeled well. Therefore, a fundamental task in modeling reservoir wells is to accurately model flow into the wellbore using larger grid sizes for full field simulations, where larger timestep sizes are preferable, and to develop an accurate well equation, which allows the calculation of bottom-hole well pressure, P_w, when the rate, Q, of production or injection is known, or the calculation of Q when P_w is known.

The first comprehensive study of this problem for cell-centered finite difference approximations on square grids was done by Peaceman in [18] for single phase Darcy flow in two dimensions. Peaceman's study presented a proper interpretation of the well-block pressure, and showed how it relates to the flowing bottom-hole pressure. The importance of this study is that the computed cell pressure has been associated with the steady-state pressure for the actual well at an equivalent radius, r_{eff}. Contrary to previous studies, which had related the computed cell pressure to the average pressure of the radial flow over the grid cell, Peaceman derived that $r_{eff} \approx 0.2h$ (here h is the

Date: December 8, 1998.

cell-size) using three different methods: (a) numerically, by solving the pressure equation on a sequence of grids and producing $r_{eff} = 0.2h$; (b) analytically, by assuming that the pressure at the adjacent block is computed exactly by the radial flow model and getting $r_{eff} = 0.208h$; (c) by solving exactly the system of difference equations and using the equation for the pressure drop between the injection and production wells in a repeated five-spot pattern given by Muskat [12] and getting $r_{eff} = 0.1987h$.

Peaceman's study was extended in various directions (including off center and multiple wells within a well-block, non-square grids, anisotropic permeability, horizontal wells, etc) by a number of numerical analysts and petroleum engineers (see, e.g. [1, 5, 13, 16, 19]). Peaceman himself has extended his study to more general situations including non-square grids and anisotropic permeability [19] and more general geometries [20]. For arbitrary location of the well we refer to [1] and for a comparative study of numerical simulation of horizontal wells we refer to [13]. To our knowledge, all existing studies have been done for cell-centered finite difference approximations of the pressure equation. On the other hand, finite element approximations have already been successfully used for groundwater flow simulation (see, e.g. [7, 8, 9]). It is apparent that, in order to use finite elements in the presence of wells, it is necessary to derive accurate well models for this important and widely used class of numerical methods.

In this paper we derive well equations for isotropic reservoirs in two different directions: (1) single phase Darcy flow with mixed finite element approximations on triangular grids and Galerkin approximations for bilinear finite elements on squares; (2) single phase high velocity (non-Darcy) flow with cell-centered finite differences on square grids, mixed finite element approximations on triangular grids and Galerkin approximations for bilinear finite elements on squares. The governing equation used to describe the non-Darcy flow is Forchheimer's correlation between the pressure gradient and the flow velocity.

High velocity fluid flow through a porous media deviates from Darcy's law, which linearly correlates pressure drop and velocity ([10, 4]). Forchheimer's quadratic relation can be applied in such cases. However, in most simulations of flow through porous media, the non-Darcy effect is incorporated through a skin coefficient (see [21]) defined only in the computational cell confining the wellbore. This coefficient is calculated from well test data [15]. The skin coefficient approach is not accurate, especially in cases of gas flow, where the fluid velocity can be sufficiently high for the non-linear behavior to appear in an extended region around the well [17].

Our analysis is based on the fundamental assumption that the flow is radial in the neighborhood of the well. Pressure dependence of the fluid physical properties and use of the quadratic Forchheimer equation introduce nonlinearities; however, the radial flow assumption can be verified for isotropic porous media (see, e.g. [2] and for more general flows [6]). Thus, our analysis can be used for quite general flow models and various numerical methods and techniques.

2. Analytical solution in the neighborhood of the well

The problem of modeling flow from a well with a radius which is substantially smaller than the discretization parameter or mesh size requires the use of analytical formulas. These formulas are only known in the case of simplified flow situations and thus constitute practical limitations in their application. We present analytical formulas for the Forchheimer flow in this section.

We consider the steady-state flow in porous media. The equation expressing the mass conservation is:

$$\nabla \cdot \vec{u} = Q\delta. \tag{2.1}$$

Here $\vec{u}$ is the mass flux, δ is point δ-function representing a well placed at the origin, and Q is the mass production/injection rate of this well. The pressure P satisfies the Forchheimer relation (see, e.g. [2, 22]),

$$-\nabla P = \rho^{-1}(\mathbf{K}^{-1}\mu + \beta|\vec{u}|)\vec{u}, \tag{2.2}$$

where $\mathbf{K}$ is the permeability tensor, which has units of [length^2], μ is the viscosity, ρ is the density, and β is a parameter with units of [length^{-1}], which is called Forchheimer's coefficient and is a porous medium property that can be measured experimentally. Generally, one may consider the following nonlinear seepage law [14]:

$$-\nabla P = \rho^{-1}(\mathbf{K}^{-1}\mu + \beta|\vec{u}|^n)\vec{u},$$

where n is a positive parameter. Obviously, this includes the linear Darcy's law $\beta = 0$ and Forchheimer's law $n = 1, \beta \neq 0$.

The basic assumption is that the flow is radial and that coefficients are constant (at least near the well). Specifically, we assume that

1. The flow is two dimensional in x and y (no gravity term);
2. $\mathbf{K}$ is a constant K times the identity matrix, i.e. $\mathbf{K} = K\mathbf{I}$;
3. β is a constant;
4. μ and ρ are constant in the neighborhood of the well;
5. The flow is radial in the neighborhood of the well.

We use the mass flux (or velocity) in order to have the production/injection rate, Q, in terms of mass instead of volume. For fluids with constant density this is equivalent to a renormalization of the equation and leads to a formulation which will directly produce the mass. We will discuss possible generalizations at the end of this manuscript.

Of the above assumptions, perhaps the most interesting is the last. It implies that the well should be circular or its size so small that the variations in its geometry can be neglected. The decay properties of the Green's function then imply that the flow becomes radial in the limit as one approaches the well (or singularity).

We derive the analytical model as follows. Assume that the well is at the origin and introduce a polar coordinate system (r, θ). If the flow is radial then the velocity $\vec{u}$ must be of the form

$$\vec{u} = w(r)(\cos\theta, \sin\theta).$$

TABLE 1. Darcy flow simulation conditions for verification of the methodology

Injection rate	$0.05\,mmscf/day$
Production rate	$4 \times 0.05\,mmscf/day$
Reservoir dimensions	$200\,ft \times 200\,ft \times 1\,ft$
Initial pressure	$5000\,psia$
Initial temperature	$300^o F$
Fluid density	$\rho = 1.78 \times 10^{-1}\,gr/cm^3$
Fluid viscosity	$\mu = 2.56 \times 10^{-2}\,cP$
Reservoir permeability	$K = 10\,mD$

Using (2.1),

$$w' + r^{-1}w = 0, \text{ for } r > 0,$$

i.e., $w = Cr^{-1}$. The constant C is proportional to Q. Since Q represents the mass injection/production rate of the well, Q is in fact the mass flux through any small circle B_ϵ centered at the origin, i.e.

$$Q = -\int_{B_\epsilon} \vec{u} \cdot \vec{n}\, ds = 2\pi C, \quad \text{or} \quad C = -\frac{Q}{2\pi}.$$

Here $\vec{n}$ is the outward normal on the circle.

The pressure, p, satisfies Forchheimer's relation (2.2) and will tend to infinity as $r \to 0$ in the case of an idealized point source well. Substituting

$$\vec{u} = -\frac{Q}{2\pi r}(\cos\theta, \sin\theta)$$

in (2.2), dotting with the vector $\vec{n} = (1, 0)$ and integrating from $(r_0, 0)$ to $(r, 0)$ gives

$$P(r) - P(r_0) = F(r) - F(r_0) \tag{2.3}$$

where

$$F(r) = \frac{K^{-1}\mu Q}{2\pi\rho}\log(r) - \frac{\beta Q|Q|}{4\pi^2\rho r}.$$

Equation (2.3) is the analytical flow model for flow near the well.

We ran several tests to verify our codes and the above model. Results are presented here from the triangular mixed finite element code runs. The conditions for the simulations are given in Table 1. The reservoir is square with four injection wells, each one located at a corner cell. One producing well is located at the center of the reservoir, which produces with a rate four times larger than each injecting well. We took advantage of symmetry and ran the code on a 100ft×100ft region with one production and one injection well with equal rates.

The absolute magnitude of the pressure cannot be determined from the analytical model since the model is only valid in the neighborhood of the well. However, we were able to fit the model to the output by aligning both curves at one point. We did this by choosing some value of r_0 (typically, $r_0 \approx 20$ft) and normalized both the computed

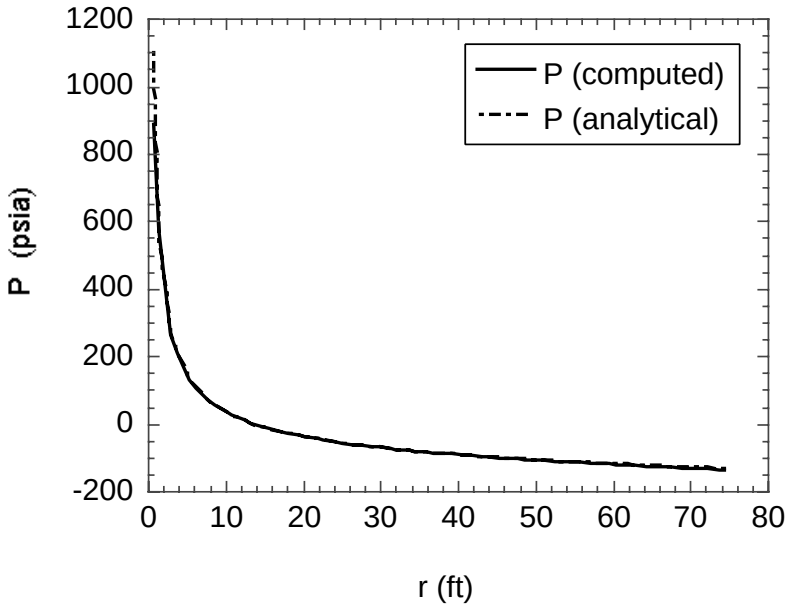

FIGURE 1. The computed and analytical normalized pressure for $\beta = 1.71 \times 10^{11} ft^{-1}$.

and analytical value to be zero there. The pressure field close to the well was then predicted with good accuracy, using the analytical model. Results from the triangular mixed finite element code near an injection well for $\beta = 1.71 \times 10^{11} ft^{-1}$ are given in Figure 1 and Figure 2. The value of the Forchheimer coefficient used in this case is at the high end of the range of the experimental data [3] in order to highlight the nonlinear effects. Since the difference between the analytical and numerical solution is difficult to see in the first figure, we include an expanded view in the second. We used a mesh size of $h = 100/60$ ft. The model and computed values agree to within 2% throughout the reported range of r (excluding $r = 0.8$). The results for the production well were identical except for a change in sign.

For comparison, Figure 3 presents the case of $\beta = 0$. Even though the differences in pressure on the computation mesh is moderate, the Forchheimer effect is much more prominent if one uses the analytical model to predict the pressure at an injection well. For example, a well with radius of 0.35ft would have a wellbore pressure of 5263psi for $\beta = 0$ and 7560psi when $\beta = 1.71 \times 10^{11} \text{ft}^{-1}$. The strong β dependence near the well is even more evident if a larger β is used.

3. A well model for cell-centered finite differences and Forchheimer flow

In this section, we derive a well model for cell-centered finite differences. The model accounts for the behavior that results from Forchheimer's term. The pressure in the cell

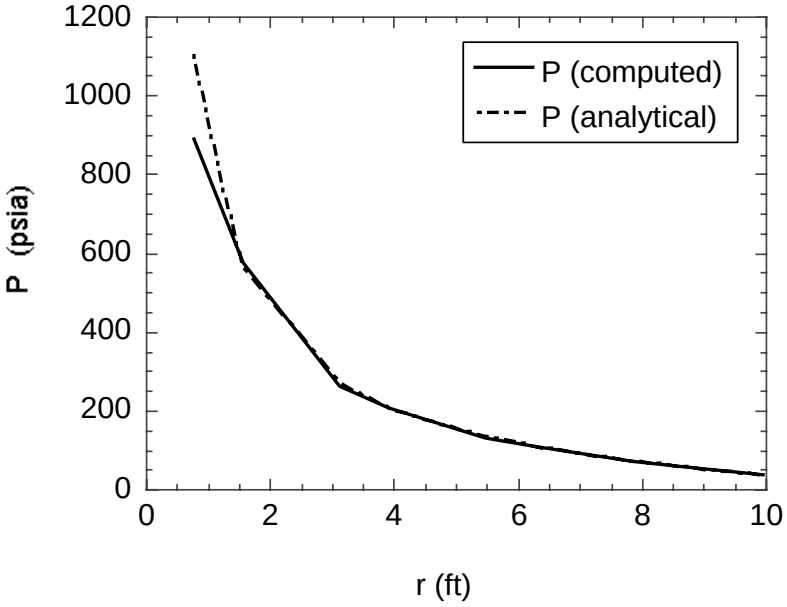

FIGURE 2. The computed and analytical normalized pressure for $\beta = 1.71 \times 10^{11} ft^{-1}$ (expanded).

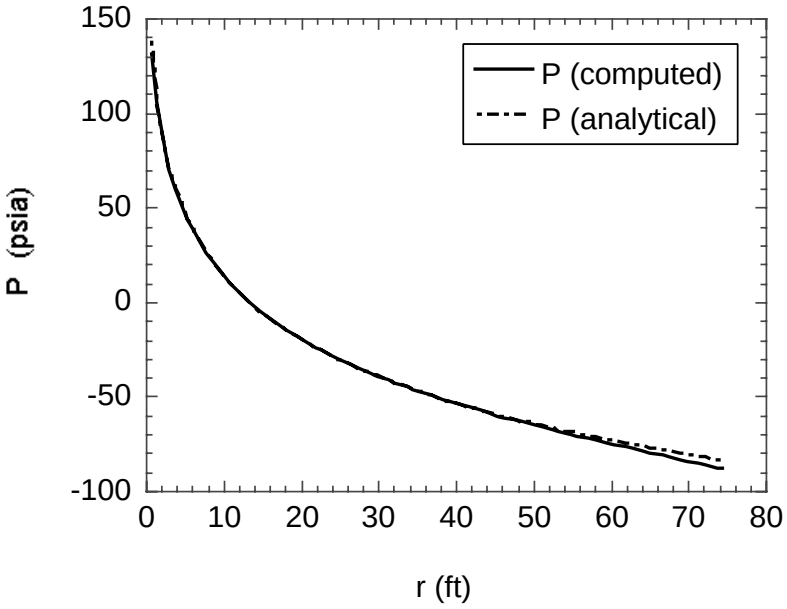

FIGURE 3. The computed and analytical normalized pressure for $\beta = 0.0$.

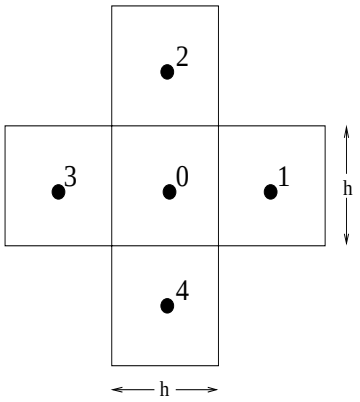

FIGURE 4. Block 0 containing a well and its four neighboring blocks

adjacent to the well-block is assumed to be accurately approximated. This is analogous to the first approach of Peaceman, described in the introduction and it reduces to Peaceman's results when $\beta = 0$.

The model of [18] is extended to include the Forchheimer effects. We consider the problem described by (2.1), (2.2) in the case when the well is located in the center of the center square of a square grid (see, Fig. 4). The cells are numbered by giving the well cell index 0 and the cell to its right index 1. Using summation by parts, the discrete equations, which result from cell-centered finite difference approximations, can be written as

$$A(P, \phi) = -Q\phi_0. \tag{3.1}$$

Here P and ϕ are vectors with dimension equal to the number of cells. The quadratic form $A(\cdot, \cdot)$ is given by

$$A(v, w) = \sum_{\mathcal{E}_{ij}} \rho(K^{-1}\mu + \beta|\vec{u}(v)_{ij}|)^{-1}(v_i - v_j)(w_i - w_j),$$

where $\mathcal{E}_{ij}$ is the edge between cells i and j. The quantity $\vec{u}(v)_{ij}$ is the normal component of the mass flux associated with the pressure vector v at the edge $\mathcal{E}_{ij}$ and satisfies Forchheimer's relation

$$\rho^{-1}(K^{-1}\mu + \beta|\vec{u}(v)_{ij}|)\ \vec{u}(v) = -\frac{v_i - v_j}{h}. \tag{3.2}$$

Taking

$$\phi_i = \begin{cases} 1 & \text{if } i = 0, \\ 0 & \text{otherwise,} \end{cases} \tag{3.3}$$

in (3.1) and using the symmetry of the solution P (i.e. $P_1 = P_2 = P_3 = P_4$) gives

$$\rho(K^{-1}\mu + \beta|\vec{u}_{01}|)^{-1}(P_0 - P_1) = -Q/4. \tag{3.4}$$

Here $|\vec{u}_{01}|$ is the mass flux throught edge $\mathcal{E}_0$ into the well cell and therefore

$$|\vec{u}_{01}| = \frac{Q}{4h}.$$

Substituting this back into (3.4) and simplifying gives

$$P_0 - P_1 = -\frac{QK^{-1}\mu}{4\rho} - \frac{Q|Q|\beta}{16h\rho}. \tag{3.5}$$

The analytical well model should be a relatively good approximation in cell 1. This means that if we are given a bottom-hole pressure P_w and a well radius r_w,

$$P_1 = P_w + F(r_1) - F(r_w). \tag{3.6}$$

Adding (3.5) and (3.6) gives

$$P_0 = P_w + F(r_1) - F(r_w) - \frac{QK^{-1}\mu}{4\rho} - \frac{Q|Q|\beta}{16h\rho}. \tag{3.7}$$

The above relation suggests that the pressure behavior near the well is significantly more complicated in the case of Forchheimer flow. In particular, the well model depends nonlinearly on Q, ρ, β and the mesh size h.

The above model reproduces Peaceman's result in the case of Darcy flow. Indeed if $\beta = 0$ then (3.7) becomes

$$\begin{aligned} P_0 &= P_w - \frac{QK^{-1}\mu}{2\pi\rho}(\log\frac{r_w}{h} + \frac{\pi}{2}) \\ &= P_w - \frac{QK^{-1}\mu}{2\pi\rho}\log\frac{r_w}{\alpha_1 h}. \end{aligned}$$

where $\alpha_1 = e^{-\pi/2} = 0.20788\ldots$. This is the exact value obtained by Peaceman in [18] under the assumption that P_1 is already a very good approximation to the analytical solution.

Introducing a new parameter, α_2, such that

$$\frac{1}{4\pi^2}\left(\frac{1}{r_w} - \frac{1}{\alpha_2 h}\right) = \frac{1}{4\pi^2}\left(\frac{1}{r_w} - \frac{1}{r_1}\right) + \frac{1}{16h},$$

gives $\alpha_2 = 4/(4+\pi^2)$. Thus, the well model (3.7) can be rewritten as

$$P_0 = P_w - \frac{QK^{-1}\mu}{2\pi\rho}\log\frac{r_w}{\alpha_1 h} - \frac{Q|Q|\beta}{4\pi^2\rho}\left(\frac{1}{\alpha_2 h} - \frac{1}{r_w}\right). \tag{3.8}$$

To get a better understanding of the numerical solution at the cell-block containing the well, we have introduced a well model (3.8) using two parameters α_1 and α_2. In order to show the influence of the Forchheimer term and to compare the results with the case of Darcy flows and Peaceman's formula where $r_{eff} \approx 0.2h$, we shall derive a

formula with one parameter $\alpha = r_{eff}/h$. The physical meaning of α is that it shows the distance from the center of the well at which the numerically calculated pressure for the wellblock is equal to the analytical pressure. We first introduce the Forchheimer number

$$Fo(x) = \frac{\beta K|\vec{u}(x)|}{\mu}.$$

The Forchheimer number defined above varies pointwise and becomes very large at the wellbore. For our purpose, we consider this quantity only at the boundary of the well cell, i.e.

$$Fo = \frac{\beta K|\vec{u}_{01}|}{\mu}.$$

Note that the total flow Q into the well cell satisfies $|Q| = 4h|\vec{u}_{01}|$ so

$$Fo = \frac{\beta K|Q|}{4h\mu}. \tag{3.9}$$

In order to develop a single parameter representation of (3.7) we look for an α such that

$$\begin{aligned} P_0 &= P_w + F(r_1) - F(r_w) - \frac{QK^{-1}\mu}{4\rho} - \frac{Q|Q|\beta}{16h\rho} \\ &= P_w + F(\alpha h) - F(r_w). \end{aligned} \tag{3.10}$$

Simple manipulations give

$$\begin{aligned} P_0 &= P_w - \frac{\mu Q}{2\pi K\rho}\left[\left(\log(r_w/h) + \frac{\pi}{2}\right) + Fo\left(\frac{2}{\pi}(1 - \frac{h}{r_w}) + \frac{\pi}{2}\right)\right] \\ &= P_w - \frac{\mu Q}{2\pi K\rho}\left[\log(r_w/\alpha h) + \frac{2Fo}{\pi}(\frac{1}{\alpha} - \frac{h}{r_w})\right]. \end{aligned}$$

This leads to the following nonlinear equation for the parameter α:

$$\frac{\pi}{2}(1 + Fo) = \ln\left(\frac{1}{\alpha}\right) + \frac{2}{\pi}Fo\left(\frac{1}{\alpha} - 1\right), \tag{3.11}$$

In the case of Darcy flow, when $\beta = 0$, the Forchheimer number is identically zero and this equation reduces to Peaceman's result $\pi/2 = \ln(1/\alpha)$ or $\alpha = \alpha_1$. In addition, as Fo tends to infinity, α tends to $\alpha_2 = 4/(4 + \pi^2)$. Clearly, the one and two parameter models are mathematically identical and only differ in the representation of the constant of integration.

In order to check the validity of the well model we have performed additional numerical simulations of the five-spot reservoir discussed earlier. A stationary state is achieved after very few time steps. Figure 5 was produced using our finite difference code applied to the $\beta = 0$ case. This code has been developed internally with Mobil Strategic Research Center and uses Numerical Analysis Objects (see [11]). It reproduces the results

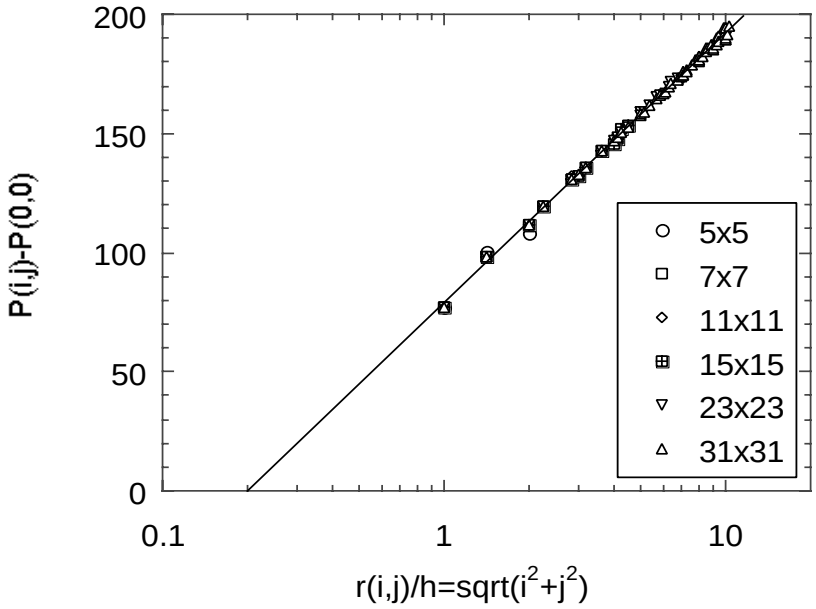

FIGURE 5. Numerical solution for pressure in a 5-spot well reservoir in the case of Darcy flow.

of Peaceman. Note that the Peaceman constant $\alpha = r_{eff}/h \approx .2h$ is given by the $y = 0$ intercept.

In Figure 6 we report the corresponding results for the case of Forchheimer flow. The physical problem is the same as the one solved for Darcy flow and described in Table 1. In order to clearly see the effects of the nonlinearities, the Forchheimer coefficient β was chosen to be $\beta = 1.71 \times 10^{11}\,\mathrm{ft}^{-1}$. The difference between the results shown on Figures 5 and 6 leads to the obvious conclusion that the use of Darcy flow equivalent radius in the case of non-Darcy flow may lead to significant errors. Instead, one should use one of the equivalent equations (3.7), (3.8), (3.10).

Figure 8 gives a plot of the solution of (3.11). At high Fo, when the non-Darcy effects are important, r_{eff} essentially does not change at $r_{eff} = \alpha_2 h \simeq 0.288h$. For $0 < Fo < 5$, there is almost a linear increase in r_{eff}. It appears that use of Peaceman's approximation of $r_{eff} \simeq 0.2h$ in simulations where Forchheimer flow is important leads to significant overestimation of P_w (for producing wells).

Empirically, the well equation model proposed here can be tested with the results of the simulation. The radial flow equation for Forchheimer flow (eqn. 3.7) can be written for the pressure drop between the well-cell and its neighboring cells as

$$\frac{(P_r - P_o)}{\frac{\mu}{k}\frac{Q}{2\pi}} = \left[\ln\left(\frac{r}{h}\right) - \frac{\beta K Q}{2\pi\rho\mu}\left(\frac{1}{r}\right)\right] - \left[\ln(\alpha) - \frac{\beta k Q}{2\pi\rho\mu h}\left(\frac{1}{\alpha}\right)\right] \tag{3.12}$$

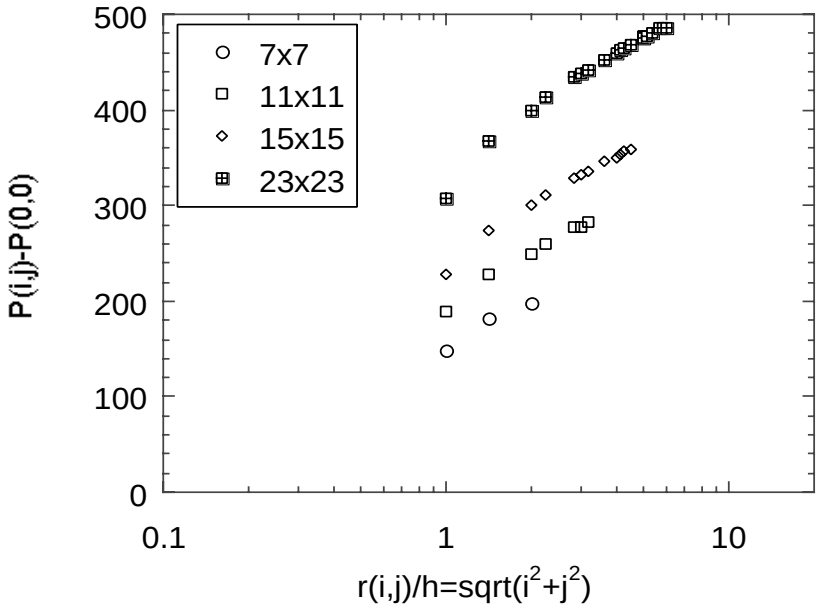

FIGURE 6. Numerical solution for pressure in a 5-spot well reservoir in the case of Forchheimer flow.

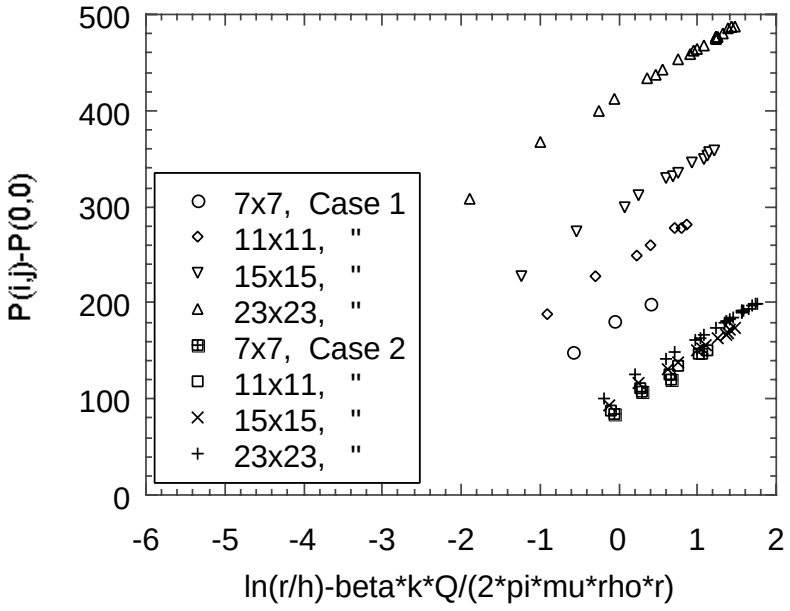

FIGURE 7. Numerical solution for pressure in a 5-spot well reservoir for Forchheimer flow. Case 1 is for $\beta = 1.71 \times 10^{11} ft^{-1}$ and case 2 is for $\beta = 1.71 \times 10^{10} ft^{-1}$

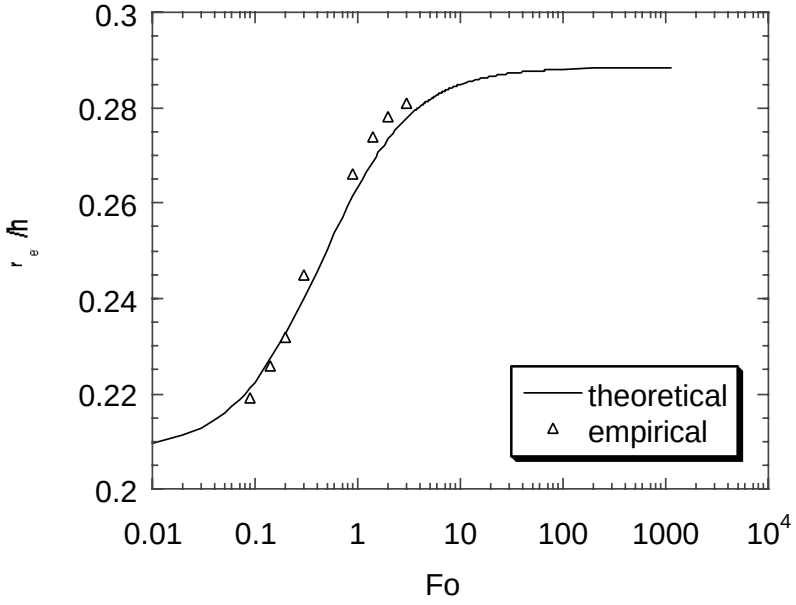

FIGURE 8. Dependence of α on Forchheimer number and comparison of the graphically obtained $\frac{r_{eff}}{h}$ for each Forchheimer number run with the theoretical curve (equation 3.11).

which means that $(P_r - P_o)$ should vary linearly with $\ln\left(\frac{r}{h}\right) - \frac{\beta k Q}{2\pi\rho\mu}\left(\frac{1}{r}\right)$. Figure 7 shows pressure differences between the wellblock and the neighboring cells obtained by numerical simulation for Forchheimer flow. The simulation data are plotted with the appropriate abscissa, as defined above, for different cases. The linear relationship is confirmed in this figure. The slope of each line does not depend on β or the discretization, as predicted by equation (3.12). The intercept with the x-axis for each run presented in Figure 7 can be used to obtain an empirical value for the ratio $\alpha = r_{eff}/h$. This empirical value for each simulation is compared in figure 8 with the theoretically obtained value of α (which can be calculated from the known Forchheimer number and equation (3.11)). The agreement is very reasonable (two significant figures) considering the crudeness of the graphical method.

4. A well model for Galerkin approximations using bilinear finite elements

In a finite element setting using bilinear finite elements on a square grid, we consider an ensemble of four finite elements sharing a common vertex with index 0 (see Figure 9). We assume that the well is placed at the vertex 0 and the flow is radial in its vicinity. We assume that bilinear finite elements have been used and the flow is radial around the well which is located at the point with index 0. For computing the finite element stiffness matrices we employ one-point quadrature (the quadrature uses the center of

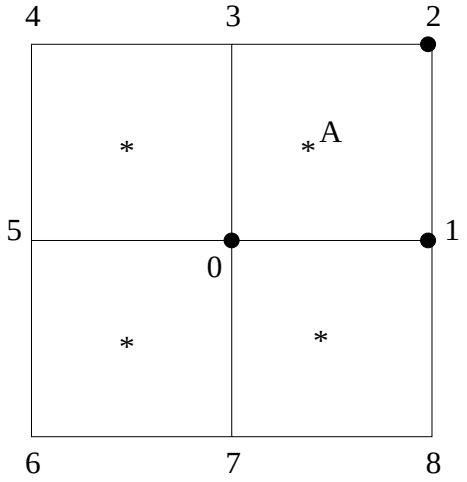

FIGURE 9. Four finite elements sharing a common vertex as a well

the finite element; in the case of element with nodal vertices 0, 1, 2, and 3 shown on Fig. 9 this is the point A).

The row in the stiffness matrix corresponding to the unknown P_0 is compiled from the integral

$$\sum_e \int_e \rho \left(K^{-1}\mu + \beta|\vec{u}|\right)^{-1} \nabla P \cdot \nabla \phi_0 \, dx = -Q, \tag{4.1}$$

where the summation is over the four finite elements sharing the vertex 0. The nodal basis function, ϕ_0, on vertex 0 has the value of one, since P and ϕ_0 are piecewise bilinear functions. We take $\vec{u}$ to be the constant $\vec{u}_e$ on the cells containing the well.

Taking into account the radial symmetry of the solution P, which result in taking $P_1 = P_3 = P_5 = P_7$ and $P_2 = P_4 = P_6 = P_8$, we get the following finite element equation corresponding to the unknown P_0.

$$\frac{4}{3}\rho \left(K^{-1}\mu + \beta|\vec{u}_e|\right)^{-1} (2P_0 - P_1 - P_2) = -Q. \tag{4.2}$$

The element (cell) velocity $\vec{u}_e$ satisfies the Forchheimer's law (instead of Darcy's law), which relates the velocity to the pressure gradient. In the case of radial symmetry, one can proceed as follows: first note that approximately we have

$$\rho^{-1} \left(K^{-1}\mu + \beta|\vec{u}_e|\right) |\vec{u}_e| \approx \frac{P_0 - P_2}{\sqrt{2}h}. \tag{4.3}$$

In order to utilize equation (4.2) we need an approximate relation of the form

$$\rho^{-1} \left(K^{-1}\mu + \beta|\vec{u}_e|\right) |\vec{u}_e| \approx \frac{P_0 - P_1}{\gamma h}. \tag{4.4}$$

TABLE 2. γ as a function of h and β.

h	$\beta = 0$	$\beta = 8.55 \times 10^{10}$	$\beta = 1.71 \times 10^{11}$
5.00	1.33	1.36	1.36
2.50	1.33	1.36	1.37
1.25	1.33	1.37	1.37

Obviously, this approximation is not valid for $\gamma = 1$ since this will give the x-derivative of the pressure at the point on a distance $0.5h$ from the well instead of distance $\sqrt{2}h/2$ where the cell-velocity $|\vec{u}_e|$ is computed. To find γ we performed a series of numerical experiments and fit the parameter. We use the same problem as described in Section 2. If the relationships (4.3) and (4.4) were true then the ratio $(P_0 - P_1)/(P_0 - P_2)$ should have a constant value approximately equal to $\gamma/\sqrt{2}$.

From Table 2, we conclude that $\gamma = 1.35$ is a reasonable approximation for this parameter. Therefore, a reasonable approximation for the Forchheimer's relation (2.2) for bilinear elements is given by

$$\rho^{-1}\left(K^{-1}\mu + \beta|\vec{u}_e|\right)|\vec{u}_e|(\gamma+\sqrt{2})h \approx |2P_0 - P_1 - P_2|. \tag{4.5}$$

We rewrite (4.2) and (4.5) in the form

$$\begin{aligned} -\frac{3}{4}Q &= \rho\left(K^{-1}\mu + \beta|\vec{u}_e|\right)^{-1}(2P_0 - P_1 - P_2), \\ |u_e|(\gamma+\sqrt{2})h &= \rho\left(K^{-1}\mu + \rho\beta|\vec{u}_e|\right)^{-1}|2P_0 - P_1 - P_2|. \end{aligned}$$

Thus, we obtain

$$|\vec{u}_e| = \frac{3}{4}\frac{|Q|}{(\gamma+\sqrt{2})h} = \frac{0.257|Q|}{h}. \tag{4.6}$$

It follows that

$$2P_0 - P_1 - P_2 = -\frac{3Q}{4\rho}(K^{-1}\mu + \beta|Q|\frac{3}{4(\gamma+\sqrt{2})h}).$$

Assuming that the well model accurately predicts the values at P_1 and P_2 gives

$$P_0 = P_w + \frac{1}{2}(F(r_1) + F(r_2)) - F(r_w) - \frac{3Q}{4\rho}(K^{-1}\mu + \beta|Q|\frac{3}{8(\gamma+\sqrt{2})h}).$$

A straightforward manipulation gives that (3.8) holds for the bilinear finite element approximation if we take

$$\alpha_1 = 2^{1/4}\exp(-3\pi/2) \quad \alpha_2 = \frac{8(\gamma+\sqrt{2})}{4(\gamma+\sqrt{2})(1+1/\sqrt{2}) + 9\pi^2}.$$

5. Mixed finite element approximation on triangular grids

In this section, we develop a well model for a mixed finite element approximation based on lowest order Raviart-Thomas on triangles. This model is motivated by considering first the case of Darcy's law. It is then extended to the case of nonzero β by making some additional assumptions. This model is similar to that developed in the case of cell centered approximations (3.8). We first consider the case of quarter-plane symmetry where the well is placed at the corner of the cell. Subsequently, we consider the case of a well which is placed at the barycenter of an interior triangle.

The mixed finite element approximation involves two approximation subspaces, V_h for velocity and Π_h for pressure. In the case of lowest order Raviart-Thomas spaces, V_h consists of piecewise linear vector functions which have continuous constant normal components. The pressure space consists of discontinuous constants. The mixed finite element approximation to (2.1, 2.2) is the pair $(u, P) \in V_h \times \Pi_h$ satisfying

$$\begin{aligned} (\rho^{-1}(K^{-1}\mu + \beta|u|)u, \psi) - (P, \nabla \cdot \psi) &= 0 \qquad \text{for all } \psi \in V_h, \\ (\nabla \cdot u, \xi) &= (Q, \xi) \qquad \text{for all } \xi \in \Pi_h. \end{aligned} \tag{5.1}$$

In the above equations, the pairing $(\cdot, \cdot)$ denotes

$$(v, w) = \int_\Omega v(x) w(x)\, dx$$

when v and w are scalar functions and

$$(v, w) = \int_\Omega v(x) \cdot w(x)\, dx$$

when v and w are vector functions.

We start with the quarter plane symmetry case and put the well at the corner opposite the hypotenuse in a square which is subdivided into two triangles by connecting the vertices adjacent to the well vertex. The well triangle will be denoted τ_1 and its neighbor is τ_2. The pressure and velocity nodes are labeled as in Figure 10.

We first consider the case of Darcy flow. As usual, the coefficients are assumed constant in the neighborhood of the well. Let ψ_i, $i = 1, \ldots, 5$, be the velocity basis functions associated with the nodes $\{x_i\}$. By symmetry, the correct boundary condition is no flow on the x and y boundary edges. This means that the solution u has zero velocity nodal components on the nodes x_1 and x_2.

It is straightforward to check that

$$(\psi_3, \psi_4) = (\psi_3, \psi_5) = 0.$$

Note that the nodal velocity function ψ_3 is given by

$$\psi_3(x, y) = \begin{cases} \frac{\sqrt{2}}{h}(x, y) & \text{for } (x, y) \in \tau_1, \\ \frac{\sqrt{2}}{h}(h - x, h - y) & \text{for } (x, y) \in \tau_2. \end{cases}$$

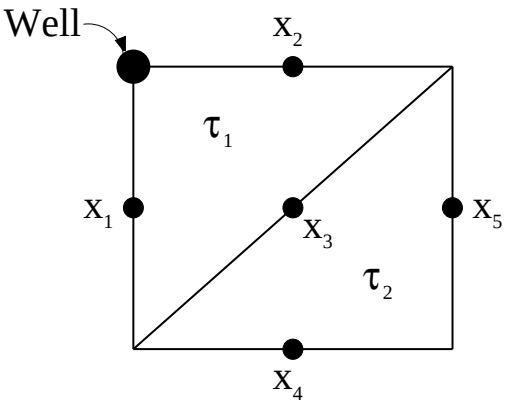

FIGURE 10. Two triangular elements forming a cell with well

This means that in the case of Darcy Flow, the solution pair (u, P) satisfies

$$\begin{aligned} \rho^{-1}K^{-1}\mu(u,\psi_3) - (P, \nabla\cdot\psi_3) &= \\ c_3\rho^{-1}K^{-1}\mu(\psi_3,\psi_3) - (P_1-P_2)\sqrt{2}h &= \\ c_3\frac{2K^{-1}\mu}{3\rho}h^2 - (P_1-P_2)\sqrt{2}h &= 0. \end{aligned} \tag{5.2}$$

Here c_3 is the coefficient of ψ_3 in the expansion of u and P_1 and P_2 are the values of P on τ_1 and τ_2 respectively. The basis function ψ_3 defined above has a constant unit normal on the edge between τ_1 and τ_2. Consequently, the total flux Q is given by

$$Q = -4\sqrt{2}hc_3. \tag{5.3}$$

Combining the two equations gives

$$P_1 - P_2 = -\frac{\mu Q}{12K\rho}.$$

To extend this to the case of non-Darcy flow, we need to make some additional assumptions. As in the bilinear finite element case, we assume that the absolute value of the velocity is constant in the cell. It is natural to take this value to be $|u_c| \equiv |u(h/2, h/2)| = |u\cdot n(h/2, h/2)| = |c_3|$. Then, equation (5.2) is replaced by

$$\begin{aligned} \rho^{-1}(K^{-1}\mu + \beta|u_c|)(u,\psi_3) - (P, \nabla\cdot\psi_3) &= \\ c_3\frac{2(K^{-1}\mu + \beta|u_c|)}{3\rho}h^2 - (P_1-P_2)\sqrt{2}h &= 0. \end{aligned} \tag{5.4}$$

Using the above relations gives

$$P_1 - P_2 = -\frac{Q}{12\rho}\left(K^{-1}\mu + \beta\frac{|Q|}{4\sqrt{2}h}\right).$$

TABLE 3. The flow through the diagonal over the total flow for a well in the barycenter of a right isoceles triangle.

h	$\beta = 0$	$\beta = 1.71 \times 10^{11}$
5.000	.34	.37
2.500	.37	.39
1.250	.38	.40
0.625	.39	.40

Assuming that the well model is valid for P_2 gives

$$P_1 = P_w + F(r_2) - F(r_w) - \frac{Q}{12\rho}\left(K^{-1}\mu + \beta\frac{|Q|}{4\sqrt{2}h}\right).$$

Here $r_2 = 2\sqrt{2}h/3$ is the distance from the well to the barycenter of the triangle τ_2. A straightforward manipulation shows that (3.8) holds for the mixed finite element approximation if we take

$$\alpha_1 = \frac{2\sqrt{2}}{3}\exp(-\pi/6) \quad \alpha_2 = \frac{12\sqrt{2}}{18+\pi^2}.$$

We next consider the case when the well is at the barycenter of a right isoceles triangle. Let the vertices of this triangle be denoted by v_1, v_2, v_3 with v_1 being the vertex at the right angle. By symmetry, the ratio of the flow through (v_2, v_3) divided by the total flow should be $\angle v_2 v_4 v_3 \,/360^\circ = .39758 \equiv \zeta$. Here v_4 denotes the well location (barycenter). To test the above assumption, we report the results of computational experiments. We consider the computational example as described in Table 1 with the following changes. We used no flow boundary conditions on a reservoir of size 100ft $\times$ 100ft and a production and injection well on a diagonal each of which were at the barycenter of a triangle approximately 25ft from the corner. As can be seen from Table 3, the ratio of the flow through the diagonal to the total flow is approximately $\zeta = .39$ on fine meshes. The difference in the case of coarser grids is attributed to the fact that the boundary conditions cause the solution to deviate from the asymptotic radial behavior.

The flow across (v_2, v_3) can be related to the mixed finite element equations in exactly the same way as was done for flow across the edge with node x_3 above. Thus, (5.2) holds for the velocity basis function c_3 associated with the node x_3 on the diagonal opposite the right triangle. However, since only part of the flow comes through (v_2, v_3), (5.3) is replaced with

$$Q = -\sqrt{2}hc_3/\zeta$$

and hence

$$P_1 = P_w + F(r_2) - F(r_w) - \frac{\zeta Q}{3\rho}\left(K^{-1}\mu + \beta\frac{\zeta|Q|}{\sqrt{2}h}\right).$$

Here $r_2 = \sqrt{2}h/3$ is the distance from the well to the barycenter of the triangle which shares the diagonal edge. This is equivalent to (3.8) if we take

$$\alpha_1 = \frac{\sqrt{2}}{3}\exp(-2\zeta\pi/3) \quad \alpha_2 = \frac{3\sqrt{2}}{9+4\zeta^2\pi^2}.$$

6. Conclusions

The accuracy of numerical simulations of flow through porous media in the presense of wells depend critically on the modeling of these wells. This problem has been studied extensively for the case of Darcy flow and simulations based on Finite Difference numerical schemes. However, there has been very limited work for simulations based on Finite Element methods. For the case of non-Darcy flow there is limited amount of work even for Finite Difference methods. The well equation used for Darcy flow and the Peaceman approximation for r_o, developed for Darcy flow, are not accurate for Forchheimer flow.

In this paper, rigorous well models were developed for Darcy flow with Galerkin Finite Elements on squares and Mixed Finite Elements on triangles. Furthermore, well equations for high velocity flow described by the Forchheimer equation were developed for Finite Difference, Galerkin Finite Element and Mixed Finite Element techniques. These equations can be used for the case of isotropic porous material and fully penetrating vertical wells. The methodology used here can be used for non-rectangular grid geometries and for other Finite Element approximations.

One significant observation from the numerical experiments is that the bottomhole well pressure is extremely sensitive to the values of the Forchheimer coefficient β. In order to accurately predict well performance for non-Darcy flow reservoir simulation, very accurate experimental and field measurements for the Forchheimer coefficient in the near wellbore region are required.

7. Acknowledgment

This work was supported in part by the EPA under Grant # R 825207-01-1, by the State of Texas under ARP/ATP grant # 010366-168 and by a gift grant from Mobil Oil Corp.

List of Symbols

$A(\cdot,\cdot)$	quadratic form (see equation 3.1)
C	constant in the solution of the radial flow equation
c_3	coefficient of the velocity basis function ψ_3
$\mathcal{E}_{ij}$	Edge between cells i and j
$F(r)$	integral of Forchheimer equation (equation 2.3)
Fo	Forchheimer number $= \frac{k\beta\rho\|u\|}{\mu}$
h	dimension of numerical cell

$\mathbf{I}$	identity matrix
K	permeability
$\mathbf{K}$	permeability tensor
$\vec{n}$	outward unit normal vector on a curve
P	pressure
Q	mass flow rate of fluid
r	direction of flow in radial flow
r_{eff}	equivalent well-block diameter
r_o	reference distance from the well
$\vec{u}$	mass flux of fluid
v	vector with components the pressure solution in all computational cells
v_1, v_2, v_3	the three vertices of a triangular element
V_h	velocity approximation subspace
w	general solution of the mass balance equation
x, y	flow directions in 2-D flow

Greek symbols

α	well equation parameter, $\alpha = r_{eff}/h$
α_1	well equation parameter associated with Darcy flow
α_2	well equation parameter associated with Forchheimer flow
β	high velocity flow or "Forchheimer" coefficient
γ	numerically evaluated parameter for Galerkin Finite Element well equation (see equation 4.4)
δ	point delta function
ζ	percentage of flow through the hypotenuse of a triangular element
θ	vectorial angle in polar coordinate system
μ	dynamic viscosity
ξ	pressure basis functions for Mixed Finite Elements
Π_h	pressure approximation subspace
ρ	fluid density
τ_i	triangular element i
ϕ	vector corresponding to delta function, defined in equation (3.3)
ψ	velocity basis functions for Mixed Finite Elements

Superscripts and subscripts

$(\,)_c$	quantity on a cell
$(\,)_e$	quantity on a cell containing the well
$(\,)_o$	quantity at the equivalent distance, r_o, from the well center
$(\,)_r$	quantity at distance r from the center of the well
$(\,)_w$	quantity at the well

References

[1] Babu, D.K., Odeh, A.S., Al-Khalifa, A.-J., and R.C. McCann, The relation between wellblock and well pressure in numerical simulation of horizontal wells - general formulas for arbitrary well locations in grids, SPE paper 20161 (June 1989).

[2] Bear, J., *Dynamics of Fluids in Porous Media*, Dover Publications, Inc., New York (1988).

[3] Coles, M.E. and K.J. Hartman, "Non-Darcy measurements in dry core and the effect of immobile liquid", SPE 39977, *SPE Gas Technology Symposium*, Calgary, Canada, (March 1998).

[4] Dake, L.P., *Fundamentals of Reservoir Engineering*, Elsevier Scientific Publiching Company, New York (1978).

[5] Ding, Y., and G. Renard, A new representation of wells in numerical reservoir simulation, *SPE Reservoir Eng.*, (May 1994), 140–144.

[6] Douglas, J., Jr., Paes Leme, P.L., and T. Giorgi, Generalized Forchheimer flow in porous media, in *Boundary Value Problems for Partial Differential Equations and Applications, Research Notes in Applied Mathematics*, (J.-L. Lions and C. Baiocchi, Eds.), v. 29, Masson, Paris, 1993, 99–113.

[7] Ewing, R.E., Simulation of multi-phase flows in porous media, Transport in Porous Media, **6** (1991), 479–499.

[8] Ewing, R.E., Recent developments in reservoir simulation, North Sea Oil & Gas Reservoirs, III (J.O. Aasen, E. Berg, A.T. Buller, O. Hjelmeland, R.M. Holt, J. Kleppe and O. Torsaeter, editors), Academic Publishers, Netherlands, 233–246 (1994).

[9] Ewing, R.E., Multiphase flow in porous media, Advanced mathematics, Computations & Applications, (A.S. Alekseev and N.S. Bakhvalov, editors), NCC Publishers, Novisibirsk, Russia, 49–63 (1995)

[10] Forchheimer, P., Wasserbewegung durch Boden, *Zeit. Ver. deut. Ing.*, **45** (1901), 1781–1788.

[11] Henderson. M.E., and S.L. Lyons, Flow in porous media using NAO Finite Difference Classes, First International Scientific Computing in Object-Oriented Parallel Environments conference, Marina del Rey, California, December 1997.

[12] Muskat, M., *The Flow of Homogeneous Fluids Through Porous Media*, McGraw-Hill Book Co., Inc. New York (1937).

[13] Nghiem L., et al., Seventh SPE comparative solution project: modeling horizontal wells in reservoir simulation, SPE Symposium on Reservoir Simulation, Anaheim, CA, Feb. 17-20, 1991.

[14] Norrie, D.H. and G. de Vries, A survey of the finite element applications in fluid mechanics, (Gallagher et al., eds), *Finite elements in fluids*, **3** Wiley, London, (1978), 363–395.

[15] Odeh, A.S., Moreland, E.E. and S. Schueler, Characterization of a gas well from one flow test sequence, *JPT*, 1500-1504, (December 1975).

[16] Palagi, C.L., and K. Aziz, Handling wells in simulators, *Proc. Fourth Intl. Forum on Reservoir Simulation*, Salzburg, Austria (1992).

[17] Papavassiliou, D.V. and S.L. Lyons, Non-darcy flow through porous media: Numerical and physical issues, *Proceedings, Institute for Multifluid Science and Technology*, 2nd annual meeting, Santa Barbara, (February 1998).

[18] Peaceman, D.W., Interpretation of well-block pressure in numerical reservoir simulation, SPE Paper 6893, Soc. Pet. Eng. J. (June 1978), *Trans. AIME*, **253**, 183–194.

[19] Peaceman, D.W., Interpretation of well-block pressure in numerical reservoir simulation with non-square grid blocks and anisotropic permeability, *Soc. Pet. Eng. J.*, (June 1983), 531–543.

[20] Peaceman, D.W., Interpretation of well-block pressure in numerical reservoir simulation - Part 3: Some additional well geometries, SPE Paper 16976 (Sept. 1987).

[21] Ramey, H.J., Non-Darcy flow and wellbore storage effects in pressure build-up and drawdown of gas wells, *JPT*, (February 1965), 23–233.

[22] Thauvin, F., and K.K. Mohanty, Modeling of Non-Darcy flow through porous media, SPE Paper 38017, *Reservoir Simulation Symposium*, Dallas, Texas, (June 1997).

Institute for Scientific Computation, Texas A & M University, College Station, Texas 77843
E-mail address: ewing@isc.tamu.edu

Department of Mathematics, Texas A & M University, College Station, Texas 77843-3368
E-mail address: lazarov@math.tamu.edu

Upstream Strategic Research Center, Mobil Technology Company, Dallas, Texas 75244
E-mail address: steve_l_lyons@email.mobil.com

Upstream Strategic Research Center, Mobil Technology Company, Dallas, Texas 75244
E-mail address: dv_papavassiliou@email.mobil.com

Department of Mathematics, Texas A & M University, College Station, Texas 77843-3368
E-mail address: pasciak@math.tamu.edu

Upstream Strategic Research Center, Mobil Technology Company, Dallas, Texas 75244
E-mail address: guan_qin@email.mobil.com